



Effects of oxidant acid treatments on carbon-templated hierarchical SAPO-11 materials: Synthesis, characterization and catalytic evaluation in *n*-decane hydroisomerization



Raquel Bértolo^a, João M. Silva^{a,b}, Filipa Ribeiro^a, Francisco J. Maldonado-Hódar^c, Auguste Fernandes^{a,*, b,d,*}, Angela Martins^{b,d,*}

^a IBB, Instituto Superior Técnico, Universidade Técnica de Lisboa, Av. Rovisco Pais, 1049-001 Lisboa, Portugal

^b Área Departamental de Engenharia Química and CIEQB, Instituto Superior de Engenharia de Lisboa, Rua Conselheiro Emídio Navarro, 1, 1959-007 Lisboa, Portugal

^c Departamento de Química Inorgánica, Facultad de Ciencias, Universidad de Granada, 18071 Granada, Spain

^d CQB, Universidade de Lisboa, Faculdade de Ciências, Campo Grande C8, 1749-016 Lisboa, Portugal

ARTICLE INFO

Article history:

Received 23 January 2014

Received in revised form 2 July 2014

Accepted 6 August 2014

Available online 15 August 2014

Keywords:

Hierarchical SAPO-11

Carbon templating

Acidity

n-decane

Hydroisomerization

ABSTRACT

Hierarchical SAPO-11 was synthesized using a commercial Merck carbon as template. Oxidant acid treatments were performed on the carbon matrix in order to investigate its influence on the properties of SAPO-11. Structural, textural and acidic properties of the different materials were evaluated by XRD, SEM, N₂ adsorption, pyridine adsorption followed by IR spectroscopy and thermal analyses. The catalytic behavior of the materials (with 0.5 wt.% Pt, introduced by mechanic mixture with Pt/Al₂O₃), were studied in the hydroisomerization of *n*-decane. The hierarchical samples showed higher yields in monobranched isomers than typical microporous SAPO-11, as a direct consequence of the modification on both porosity and acidity, the later one being the most predominant.

© 2014 Elsevier B.V. All rights reserved.

1. Introduction

Zeolites and zeotype materials like silicoaluminophosphates (SAPO), owing crystalline frameworks and ordered networks of micropores (<2 nm), have been widely used as important heterogeneous catalysts in industrial processes such as oil refining, petrochemistry and also as adsorbents in purification and separation processes. These vast applications emerge due to the particular combination of properties of this class of materials: large surface area and crystallinity, high adsorption capacity, tailored acidity, high thermal stability, well defined pore sizes and excellent shape selectivity [1,2]. However, with an increasing need for faster diffusion rates and higher conversion of bulky molecules, the solely

microporous character of these materials can be a drawback. Indeed, reactants and products with sizes above the micropore dimensions cannot diffuse in and out of the crystals, causing loss of activity and selectivity with consequent reduction in the lifetime of the catalyst. One of the strategies to overcome this limitation is the introduction of an additional pore system (meso or macroporous) in order to fabricate hierarchically structured materials. Through this way, a single material would possess the catalytic features of micropores and the enhanced access and transport properties of mesopores [3]. The preparation methods for hierarchical materials comprise two different methods: (i) post-synthesis procedures, such as dealumination or desilication, where the mesoporosity is formed as a consequence of Al or Si extraction in acid or basic medium, or (ii) by adding one or more templates during the crystallization process. Several materials can be used as solid templates such as resins, polymers, polyurethane foams or cellulose [4]. However, the most general and versatile approach is to employ different types of porous carbons like carbon particles. In fact, the carbon templating method can be tuned to yield either nanosized zeolite crystals or mesoporous zeolite crystals. By only slightly changing the crystallization conditions it is possible for zeolite crystals to nucleate not only inside the carbon matrix but also to continue

* Corresponding author at: Área Departamental de Engenharia Química, Instituto Superior de Engenharia de Lisboa, Rua Conselheiro Emídio Navarro, 1, 1959-007 Lisboa, Portugal. Tel.: +351 218317000; fax: +351 218317001.

** Corresponding author at: IBB, Instituto Superior Técnico, Universidade Técnica de Lisboa, Av. Rovisco Pais, 1049-001 Lisboa, Portugal. Tel.: +351 21419183; fax: +351 218419198.

E-mail addresses: auguste.fernandes@ist.utl.pt (A. Fernandes), amartins@deq.isel.ipl.pt (A. Martins).

their growth through the surrounding carbon pore system in such a way that the crystals encapsulate part of the carbon matrix [5].

Although the production of hierarchical materials is most developed for zeolites, other similar materials such as SAPOs are also being studied due to its particular catalytic properties, especially when mild acidity is required. SAPO-11 (AEL topology) comprising one-dimensional, non-intersecting 10-membered ring channels with elliptical pore-apertures of $4 \times 6 \text{ \AA}$ was first reported by Lok et al. [6]. Due to its moderate acidity and suitable pore size, SAPO-11 loaded with a trace amount of noble metal has been found highly active and selective for the hydroisomerization of long chain *n*-paraffins to produce high quality diesel fuel and lubricants, achieving high isomerization yields and less cracking products [7]. The hydroisomerization of long chain *n*-paraffins over metal loaded catalysts is supposed to proceed via a bifunctional mechanism as suggested by Martens et al. [8], where the adsorption and reaction takes place at the external surface of the crystals and at the pore mouths of the 10-ring tubular pore molecular catalyst such as MCM-22 or SAPO-11 [9]. Therefore, the more pore mouths participating in the reaction and the larger external surface of the catalyst are advantageous in order to get high selectivity towards isomerization products.

The purpose of this work is to explore the catalytic behavior of hierarchical SAPO-11 materials, using a commercial Merck carbon as solid template. The surface chemistry of the carbon was modified through oxidant acid treatments and the possible interaction with SAPO-11 gel synthesis was explored, in order to study its influence on the physicochemical properties and catalytic behaviour of hierarchical SAPO-11 materials.

The bifunctional catalysts were prepared by mechanically mixing SAPO-11 samples with Pt/Al₂O₃ (final loading 0.5 wt.% Pt) in order to present the same metal function properties. These catalysts were evaluated in the hydroisomerization of long chain *n*-alkane using *n*-decane as reactant.

2. Experimental

2.1. Samples preparation

Conventional SAPO-11 sample was prepared by hydrothermal synthesis according to a previous procedure [6], with the following molar composition: 1.0 Al₂O₃: 1.0 P₂O₅: 0.4 SiO₂: 1.5 DPA: 50 H₂O. The following reagents were used as received: pseudoboehmite (Plural SB from Condea, 75 wt.% Al₂O₃), orthophosphoric acid (H₃PO₄ from Merck, 85 wt.% aq. solution), silica (AS40) as sources of T atoms and dipropylamine DPA (from Aldrich, 99 wt.% aq. solution) as structure-directing agent.

In order to study the influence of the concentration of oxygen surface groups present on the commercial carbon and their possible interaction with SAPO-11 synthesis gel, Merck carbon template was submitted to a wet oxidation treatment. A 4.6 M solution of HNO₃ was used as oxidizing agent and mixed with the carbon sample (1 g of carbon/10 mL of solution) [10]. The suspension was evaporated at 60 °C until dryness. After the acid treatment, the sample was washed with distilled water until the pH was the same as the one for distilled water. This sample will be referred to as Mox hereafter. Then, Mox sample was treated at 300 °C (5 °C min⁻¹, N₂ flow, 10 L h⁻¹) to give Mox300 material with intermediate oxygenated surface properties (partial oxygen removal).

The hierarchical SAPO-11 samples were prepared following the same procedure and molar composition used to obtain the conventional one but the method of solid templating was applied to produce hierarchical samples. In this study, three distinct carbon samples were used: the commercial Merck and two oxidized ones (Mox and Mox300).

Each carbon template (6 wt.%) was added to the gel after DPA. The latter was then transferred into an autoclave. In all cases, crystallization was achieved at 200 °C for 24 h. The products obtained were recovered by centrifugation, washed several times with distilled water and dried at 110 °C overnight. The organic and carbon templates were removed by calcinations, first at 350 °C for 2 and then at 600 °C for 12 h under air (15 L h⁻¹ g⁻¹). The obtained samples were named as S-x, where x represents the carbon template used.

2.2. Samples characterization

The structural characterization of the parent and hierarchical SAPO-11 samples was carried out with a D8 Advance diffractometer from Bruker, equipped with a graphite monochromator using Cu-K α radiation as incident beam. The powder XRD patterns were obtained from 5 to 40° (2 θ), a step of 0.03 and a time per step of 4 s. Chemical analysis of samples calcined was done by ICP-AES for Al and P contents and atomic absorption spectroscopy (AAS) for Si.

Thermogravimetric (TG) and differential scanning calorimetry (DSC) analysis were performed on a TG-DSC 92 Setaram Instrument. Each sample was heated between 25 and 900 °C (10 °C min⁻¹) under air flow (30 mL min⁻¹).

Textural characterization of the solids was carried out by means of N₂ sorption measurements isotherms at -196 °C, performed in an automatic apparatus Micromeritics ASAP 2010, where the samples were outgassed at 350 °C under vacuum before N₂ sorption measurements. The morphology and size of the crystals were analyzed by Scanning Electron Microscopy (SEM), performed on a Hitachi S400 microscope.

²⁷Al, ³¹P and ²⁹Si MAS NMR spectra were recorded in Bruker Avance III 400 NMR spectrometer (B0 = 9.4 T) at, respectively, 13, 12 and 5 kHz with 60 s recycle delays. Chemical shifts are quoted in ppm.

The samples acidity was characterized by pyridine adsorption followed by IR spectroscopy on a Nicolet Nexus spectrometer. The samples were pressed into thin wafers (10–20 mg cm⁻²) and pre-treated in an IR quartz cell at 450 °C for 3 h under secondary vacuum (10⁻⁶ mbar). The samples were then cooled down to 150 °C and contacted with pyridine ($P_{\text{eq}} = 2$ –3 mbar) during 10 min. After that, the excess of pyridine was evacuated for 30 min under secondary vacuum and then IR spectra were recorded (64 scans with a resolution of 4 cm⁻¹). The background spectrum, always recorded under identical conditions without sample and performed before each spectrum acquisition, was automatically subtracted. For quantification purposes, the spectrum of the sample after pretreatment was subtracted from the spectra obtained after pyridine adsorption and subsequent desorption.

The surface chemistry of the carbon materials was characterized by determining the point of zero charge (pH_{pzc}). In brief, a certain amount of the carbon was dispersed into an appropriate amount of CO₂-free distilled water (0.05 g cm⁻³). The slurry was then kept in a plastic bottle and shaken periodically for 2 days until the pH had stabilized, the final slurry pH value measured (glass electrode from micropH2000, Crison) corresponding to the pH_{pzc} value of the carbon matrix [11].

2.3. Preparation of bi-functional catalysts and catalytic tests

The *n*-decane hydroisomerization was carried out at atmospheric pressure in a flow reactor using 0.1 g of catalyst loaded with 0.5 wt.% of Pt. The metal function was introduced by mechanically mixing the necessary amount of Pt/Al₂O₃, (1 wt.% Pt, Aldrich) to SAPO-11 samples in order to obtain a bifunctional Pt/SAPO-11 with 0.5 wt.% metal loading. After mixing for 1 min in an agatha mortar the resulting powder was slightly pressed into wafers and

then crushed and mixed again. This procedure was repeated twice and then the powder was transferred to the catalytic reactor. Prior to the catalytic tests the samples were reduced *in situ* under H₂ flow at 500 °C for 3 h. The reaction was performed with a molar ratio H₂/n-C₁₀ = 7. The total conversion was changed by varying the reaction temperature (280–330 °C) and WHSV (6.6–13.1 h⁻¹). The reaction products were analyzed on-line with a gas chromatograph Hewlett-Packard 6890 series equipped with a flame ionization detector and a capillary CP-Sil5 column.

3. Results and discussion

3.1. Characterization of the carbon matrixes

The results from thermogravimetric measurements (nitrogen atmosphere) performed for samples Mox, Mox300 and Merck are presented in Table 1. Logically, the most oxidized Mox sample presents a very high weight loss (ca. 20%), followed by the intermediate Mox300 (11%) and finally Merck (about 4%), meaning that oxidant treatment enriched the carbon surface with oxygenated species (Mox), while subsequent thermal treatment tends to reduce the amount of poorly stable oxygenated species (Mox300) until reaching a material with no or little OSG groups, i.e. the initial Merck carbon. Therefore, the OSG percentage in our samples follows the order: Mox > Mox300 > Merck (see values in Table 1).

The changes of the surface chemistry as a consequence of oxidant acid treatments were monitored by means of pH_{pzc} measurements and the results obtained are displayed in Table 1. As it can be observed, the most oxidized sample Mox presents a pH_{pzc} value significantly lower when compared with the untreated Merck carbon, denoting a higher concentration of acidic OSG. On the other hand, sample Mox300 shows an intermediate value.

The quantitative assessment of the micropores volume, V_{micro}, and the external surface area, A_{ext}, of the samples was done applying the t-method while the mesopores volume, V_{meso} was calculated as the difference between total volume and V_{micro}. The results are reported in Table 1. One can see that oxidized sample Mox shows a decrease of V_{micro} together with an increase of both V_{meso} and A_{ext}, when compared with Merck commercial carbon, in agreement to what was previously reported [10]. This observation can be easily explained by a synergetic effect corresponding to, in one hand, the formation of OSG groups within the micropores blocking them and, in the other hand, a partial mechanical destruction of the micropores walls leading to mesopores and/or macropores development.

Upon thermal treatments in inert atmosphere, an increase in V_{micro} is observed for Mox300 sample, as OSG that were filling the micropores are partially removed. The release of OSG from the newly mesopores/macropores created (see above) might also lead to a progressive pore opening. However, in order to confirm the presence of larger macropores, mercury porosimetry experiments should be performed.

3.2. Characterization of hierarchical SAPO-11 materials

The data obtained from chemical analysis (not shown) reveal that the T atom molar fraction was similar for all SAPO-11 samples (Al_{0.50}P_{0.44}Si_{0.06}O₂). These values are normally indicative of SM2 (Si

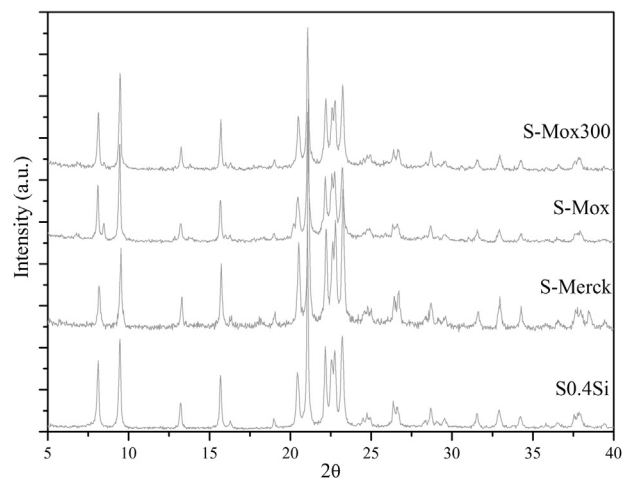


Fig. 1. XRD patterns of the samples SAPO-11 synthesized (S0.4Si) and S-Merck, S-Mox and S-Mox300 (with carbon template).

for P) substitution mechanism. One can see that Si amount incorporated during gels crystallization seems to be independent from the presence of carbon matrix.

All the samples present diffraction lines corresponding to AEL phase (Fig. 1), as reported in the literature [6]. However, the samples prepared with carbon matrixes present a slight decrease of the peaks and a slight increase of the baseline, due to the presence of a very broad band. This is consistent with the presence of well crystalline SAPO-11 materials together with an amorphous phase corresponding to the carbon matrix added during the gel preparation. Also, the absence of any other extraneous phase (alumina, aluminophosphate, etc.) is confirmed by NMR results (see below). In some cases, an extra peak at about 8.5 in 2θ corresponding to SAPO-31 contaminant phase appears, though with a very low intensity. Fig. 2.

The TG-DSC results for all SAPO-11 samples, displayed on Table 2, indicate two main weight losses corresponding to, respectively: desorption of physisorbed water (below 170 °C) and decomposition/oxidation of both DPA template and carbon matrix (170–700 °C). Assuming a theoretical DPA weight loss of about 8% for pure SAPO-11 [12], the amount of carbon matrix present in the final materials can be determined as the difference between total weight loss and estimated DPA + experimental water weight losses contributions. As it can be seen on Table 2, the total weight loss, and consequently the carbon weight loss, is similar, for the same percentage of carbon, with Merck and oxidized carbon matrixes.

The textural parameters of SAPO-11 and hierarchical SAPO-11 are quoted in Table 2. The samples prepared using carbons as templates present a value for V_{micro} characteristic of SAPO-11 structure, meaning that the original microporous structure of SAPO-11 was preserved. However, an increase of A_{ext} and V_{meso} is clearly shown in all cases regarding S0.4Si, leading to the conclusion that hierarchical materials were successfully obtained. The stronger development of this parameter was obtained for S-Merck sample. Indeed, neither the oxidation nor the following thermal treatment provokes such increase. Nevertheless, these treatments significantly influence the morphology of final SAPO-11 materials. SEM

Table 1

Amount of H₂O and OSG (oxygenated surface groups) from TG experiments and pH_{pzc} values and textural parameters for carbon matrix samples.

Samples	H ₂ O (wt.%)	OSG (wt.%)	pH _{pzc}	A _{ext} (m ² g ⁻¹)	V _{micro} (cm ³ g ⁻¹)	V _{meso} (cm ³ g ⁻¹)
Mox	7.0	20	2.99	115	0.34	0.14
Mox300	2.6	11	3.72	56	0.48	0.10
Merck	0.7	4	7.02	62	0.52	0.11

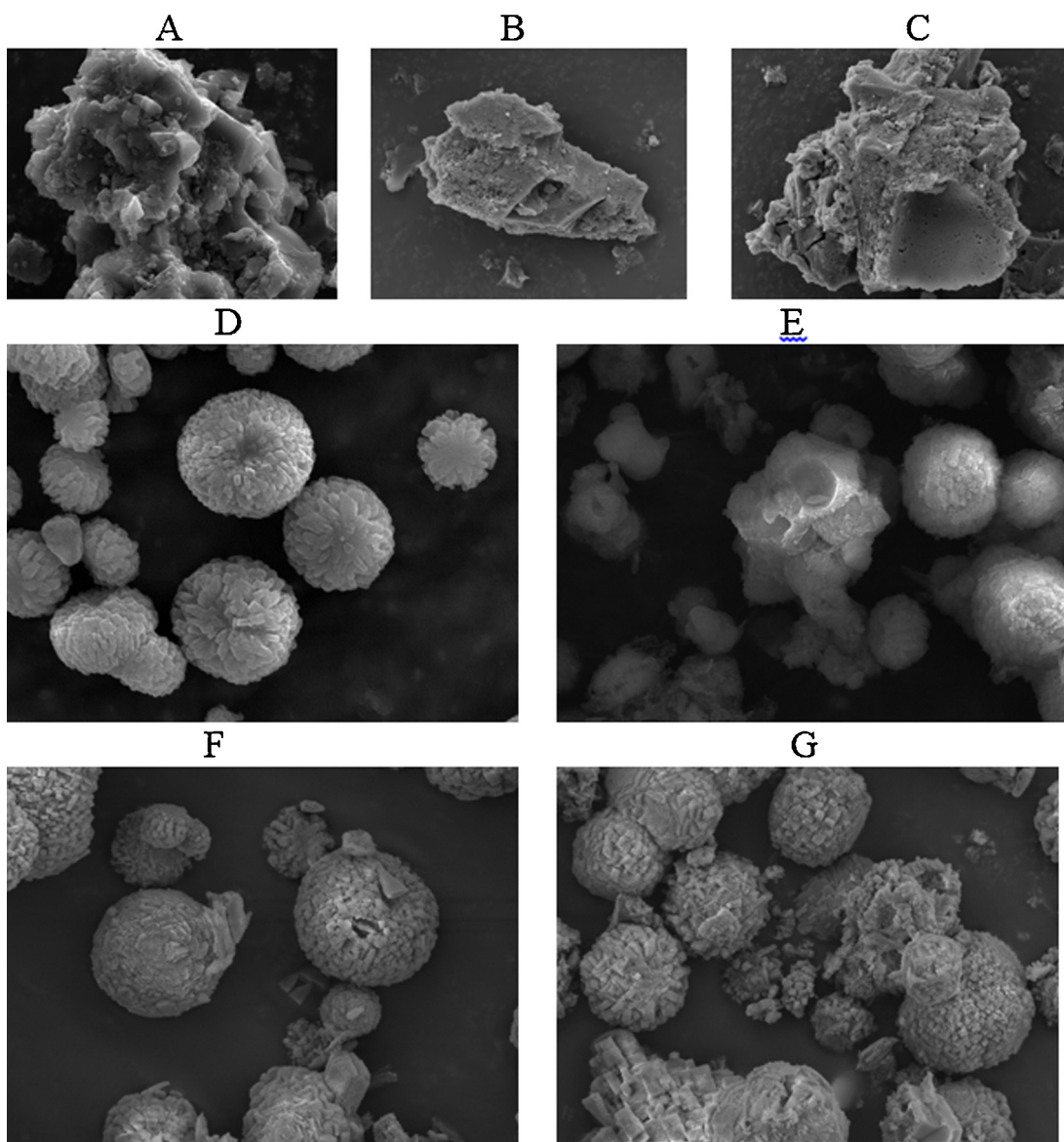


Fig. 2. SEM of carbon templates, Merck (A), Mox (B), Mox300 (C) (— 5 μm), and SAPO-11 samples, S0.4Si (D), S-Merck (E), S-Mox (F) and S-Mox300 (G) (— 5 μm).

micrographs of the different carbon matrixes and respective SAPO-11 materials are presented in Fig. 1. As can be observed, the oxidized carbons (images B and C) present more fragmented particles, especially when the oxidation is followed by heat treatment. Concerning carbon-templated SAPO-11 materials, the ordered spherical aggregates presented for S0.4Si (image D) become more heterogeneous and fragmented, with presence of large cavities, due to carbon combustion (image E). Samples prepared from oxidized carbons seem to follow the same patterns as their correspondent carbon templates, as the fragmentation and heterogeneity tend to increase from S-Mox to S-Mox300 (images F and G).

NMR spectroscopic measurements were performed in order to evaluate the structural properties of the materials synthesized and the distribution of Si, ^{27}Al , ^{31}P (sample S0.4Si) and ^{29}Si (samples S-Mox (a), S-Merck (b) and S0.4Si (c)) spectra are presented in Figs. 3 and 4, respectively. The NMR measurements were performed onto calcined, rehydrated samples. The ^{31}P spectrum of sample S0.4Si (Fig. 3a) shows two well-defined signals at about –29.2 (the most intense) and –23.2 ppm. In the ^{27}Al spectrum (Fig. 3b) four signals can be observed at 39.1, 28.0, 7.1 and –15.2 ppm (the first signal being the most intense). All these ^{27}Al and ^{31}P signals have been observed in crystalline SAPO-11 materials by other authors

Table 2

Weight losses (wt.%) observed from TG experiments, pyridine quantification (at 150 °C) and textural parameters for SAPO-11 (carbon-free and hierarchical) samples.

Sample	Weight loss (wt.%)		PyH^+ ($\mu\text{mol g}^{-1}$)	PyL ($\mu\text{mol g}^{-1}$)	A_{ext} ($\text{m}^2 \text{g}^{-1}$)	V_{micro} ($\text{cm}^3 \text{g}^{-1}$)	V_{meso} ($\text{cm}^3 \text{g}^{-1}$)
	Total	Carbon					
S0.4Si	8.3	–	46	49	21	0.07	0.04
S-Merck	35.9	26.8	17	34	47	0.06	0.10
S-Mox	32.7	23.3	31	33	40	0.07	0.08
S-Mox300	35.9	25.2	21	38	32	0.07	0.07

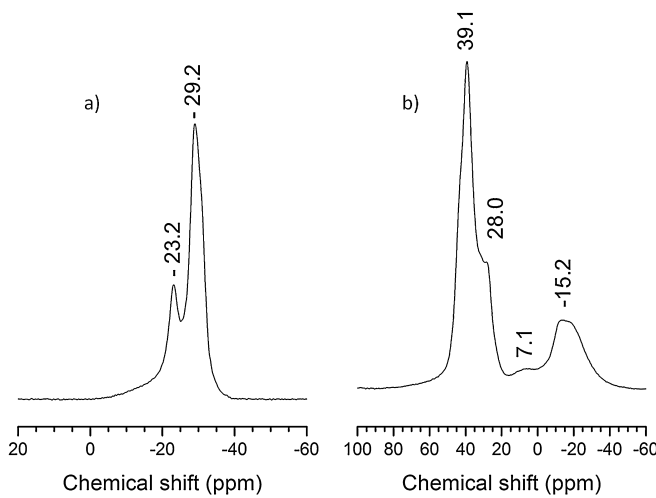


Fig. 3. ³¹P (a) and ²⁷Al (b) MAS NMR spectra of the sample S0.4Si calcined.

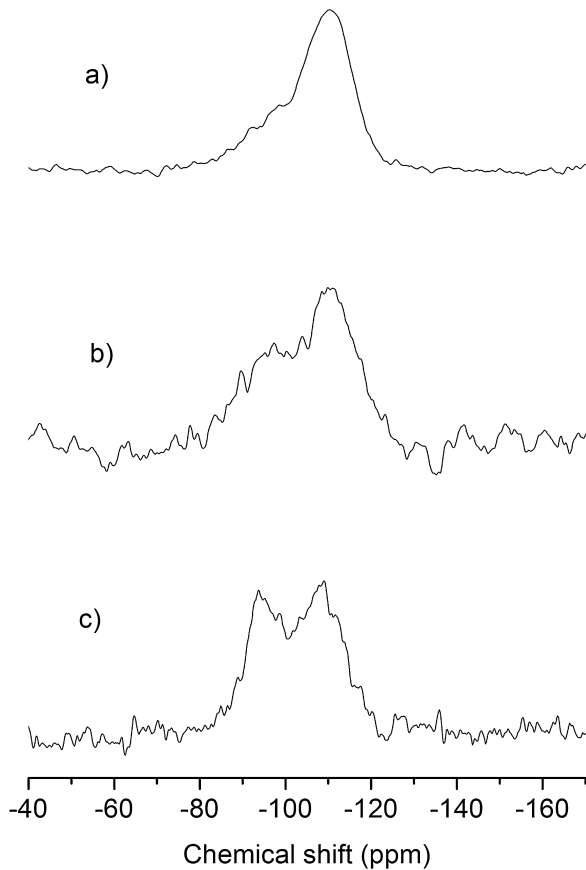


Fig. 4. ²⁹Si MAS NMR spectra of the samples S-Mox (a), S-Merck (b) and S0.4Si (c) calcined.

[13,14]. The results are well consistent with crystalline SAPO-11 materials in their hydrated form, with two different tetrahedral Al (39.1 and 28.0 ppm) and P (-29.2 and -23.2 ppm) crystallographic positions, while ²⁷Al signals at about 7.1 and -15.2 ppm are related to penta $\text{AlO}_4(\text{H}_2\text{O})$ and hexacoordinated $\text{AlO}_4(\text{H}_2\text{O})_2$ Al species, respectively. In fact, no signal from extraneous phase, namely neither γ -alumina nor amorphous aluminophosphate is observed in our samples, but instead the signals observed are a consequence of a strong water adsorption within SAPO structure [14].

The acidity of conventional SAPO-11 materials was evaluated by infrared spectroscopy (FTIR) using pyridine (Py) as probe

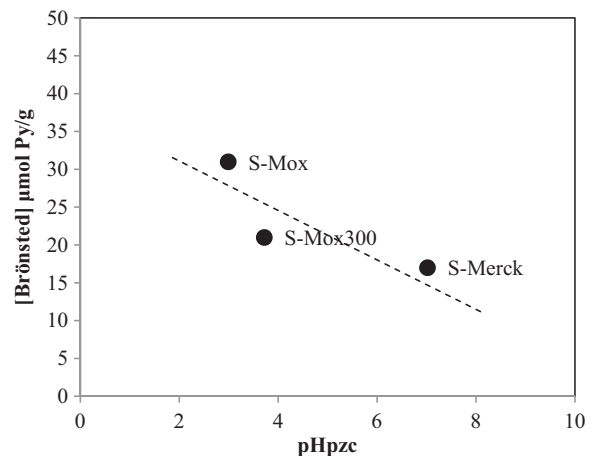


Fig. 5. Concentration of Brønsted acid sites (at 150 °C) of S-Mox, S-Mox300 and S-Merck samples as a function of pH_{pzc} values of the corresponding carbon templates.

molecule. After Py adsorption, all the samples present, in the region 1400–1700 cm⁻¹, the bands characteristic of PyH⁺ species at around 1545 cm⁻¹ (Brønsted acid sites) and coordinated PyL at ca. 1455 cm⁻¹ (Lewis acid sites) (spectra not shown).

Table 2 displays the acid concentration for parent and hierarchical SAPO-11 samples, calculated from the integrated area of PyH⁺ and PyL bands using the values of the molar extinction coefficients of the bands ($1.67 \text{ cm } \mu\text{mol}^{-1}$ for PyH⁺ and $2.22 \text{ cm } \mu\text{mol}^{-1}$ for PyL) determined by Emeis [15]. The addition of the carbon templates causes some decrease on the acid sites concentration (Brønsted and Lewis), when compared with parent S0.4Si sample. These results may suggest a possible interaction between the carbon template and the SAPO-11 precursors present in the synthesis gel, giving rise to different Si distribution for each sample, since the Si content in the final materials is approximately the same for all samples.

In order to further investigate the relationship between the surface groups of the carbon material and the acidity of the correspondent SAPO-11 materials, Fig. 5 displays the concentration of Brønsted acid sites (at 150 °C) of SAPO-11 as a function of pH_{pzc} values of the carbon templates.

It can be clearly observed a correlation between the two parameters as the higher pH_{pzc} value the lower the acidity, demonstrating once again the influence of the carbon surface chemistry on the final acidity properties of the hierarchical SAPO-11 materials.

One of the characteristics that have been reported on solid templating is that the matrixes are thought to be chemically inert and, thus, the chemical composition of the hierarchical materials can be properly optimized in the gel synthesis composition, without influence of the template [16]. However, Zhang et al. [17] reported modifications in the acidity for the solid-templated materials, arguing for a loss of crystallinity of the final materials. These results point out that the surface chemistry of the template might be an important factor to be taken into account to better understand the chemical properties of the hierarchical materials synthesized with the help of carbon templates.

3.3. n-Decane hydroisomerization

The hydroisomerization of long chain *n*-paraffins is an important process for production of diesel fuels. The diesel quality is related to its composition in linear paraffins and cetane number, increasing with the length of chain but decreasing with branching. Therefore is important that the hydroisomerization catalyst favors monobranched products and minimize cracking reactions through adequate topology and size as well as acid strength. Several authors

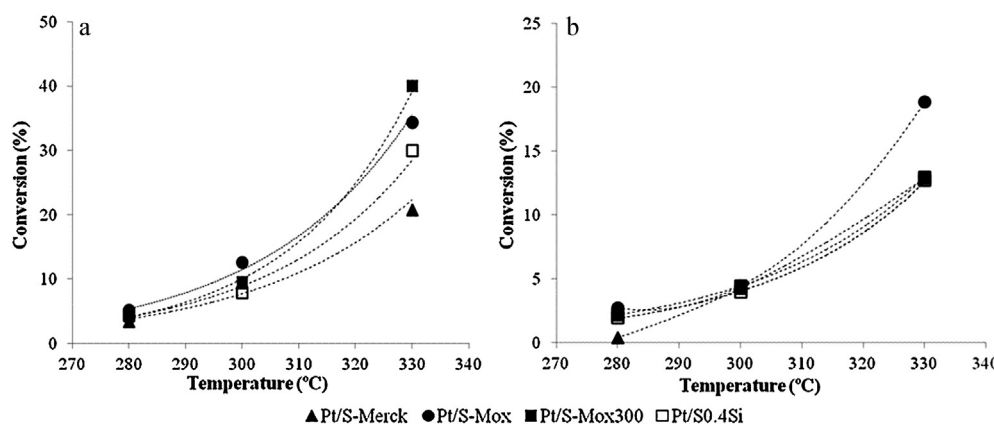


Fig. 6. Conversion of *n*-decane on $\text{Pt}/\text{Al}_2\text{O}_3 + \text{SAPO-11}$ samples catalysts at $\text{WHSV} = 6.6 \text{ h}^{-1}$ (a) and 13.1 h^{-1} (b). Reaction conditions: 0.1 g of catalyst (0.5 wt.\% of Pt), $P = 1 \text{ atm}$, molar ratio $\text{H}_2/\text{n-C}_{10} = 7$.

show that a bifunctional SAPO-11 catalyst is suitable for performing this reaction, exhibiting a high amount of isomerization products, especially monobranched isomers [7,18–21].

In this study the hydroisomerization of long-chain *n*-alkanes was performed on conventional and hierarchical bifunctional Pt/SAPO-11 catalysts, using *n*-decane as a model molecule, since it has a number of carbons sufficiently large to simulate the most important types of mechanisms that occur with long chain *n*-alkanes. The stability of the catalysts was studied by performing some previous essays with time on stream during 60 min, at constant WHSV and temperature ($\text{WHSV} = 6.6$ and $T = 280^\circ\text{C}$). The results showed that during the reaction time no important deactivation phenomena took place. Nevertheless, in order to account for some initial deactivation, each data point was acquired after 20 min time-on-stream, which allowed studying the catalysts behavior under similar deactivation state. The metal function was introduced by mechanically mixing with $\text{Pt}/\text{Al}_2\text{O}_3$ the activity of this was studied varying the reaction temperature (280°C and 300°C) and WHSV (6.6 – 13.1 h^{-1}). The results showed that the $\text{Pt}/\text{Al}_2\text{O}_3$ by itself is inert to hydorisomerization of *n*-decane, since the conversion was only 0.5%.

Fig. 6 shows the evolution of total conversion of *n*-decane with the reaction temperature for the space velocities of 6.6 and 13.1 h^{-1} . As expected, the conversion for all samples increased at higher temperature and lower space velocity. Additionally, the conversion values obtained for the hierarchical catalysts are generally slightly higher when compared with Pt/S/0.4Si.

A further exploration of the catalytic results is presented in Table 3 taken as an example the experiment performed at 300°C and WHSV of 6.6 h^{-1} . The option to deepen the study at these experimental conditions aims the comparison of the catalytic behavior at approximately iso-conversion (around 10%). Additionally, the evaluation of the catalytic behavior at low conversion, where the kinetic control of the reaction is verified, prevents the effects caused by the extensive occurrence of secondary transformations, along with diffusional or thermal interference.

As previously mentioned, the hierarchical catalysts present a slightly higher conversion when compared with conventional SAPO-11 sample, Pt/S/0.4Si. This can be attributed to the mesoporosity developed as a consequence of the solid templating method used during synthesis, which promotes a faster diffusion of the reaction intermediates. Among the three hierarchical catalysts the effect of the acidity is also relevant since Pt/S-Mox, with the higher concentration of Brønsted acid sites (see Table 2), presents also the highest catalytic conversion.

The pattern of products distribution (Table 3), was found common for all catalysts, with *n*-decane converted into monobranched

(M) and dibranched (B) isomers and also some cracking products (C), which is in accordance with the typical distribution obtained for Pt/SAPO-11 catalysts [18,19].

The results show that all samples favor the formation of 3-, 2-methylnonane and 3-ethyloctane. On the other hand, 4- and 5-methylnonanes are formed in fewer amounts. The distribution of cracked products is asymmetric in some samples, e.g. C₄ products exceeding C₆ products; this should be due to the occurrence of secondary cracking reactions. However, in all samples the isopentane is the major cracking product formed by direct scission of *n*-decane.

As can be observed from Table 3, despite the higher conversion of Pt/S-Mox, undesired products such as dibranched isomers and, especially cracking products are present in higher amounts, when compared to the other catalysts, due to the higher acidity of this sample, meaning that the simultaneous higher V_{meso} and acidity are not advantageous for the production of desired monobranched isomers.

The ratio between the sum of the yields into mono and dibranched isomers (M/B) as well as the ratio between the yields in total isomerization and cracking (I/C) is displayed on Fig. 7. The obtained results show an increase in both M/B and I/C ratios, as desired, only in the case of Pt/S-Merck.

Fig. 8 illustrates the relationship between I/C ratio and the two parameters that influenced the product distribution: concentration of Brønsted acid sites and V_{meso} .

As can be observed there is a joint effect of both mesoporosity and acidity that leads to a higher production of isomers, especially monobranched, ones and limiting the occurrence of cracking reactions (higher I/C ratio) on Pt/S-Merck catalysts. Indeed, besides all carbon template samples present V_{meso} about two times higher than that of conventional SAPO-11 material, there is a slight increase in the

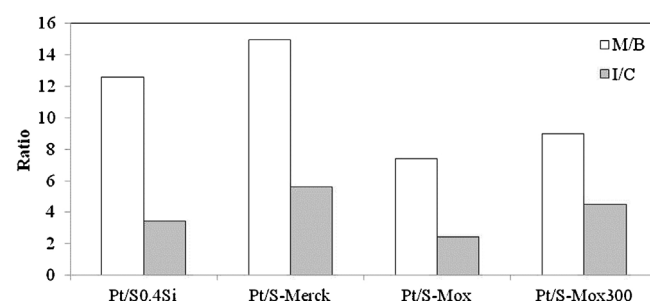


Fig. 7. Ratio of the sum of the yields into monobranched and dibranched isomers (M/B) and isomerization and cracking products (I/C) on $\text{Pt}/\text{Al}_2\text{O}_3 + \text{SAPO-11}$ samples catalysts at $\text{WHSV} = 6.6 \text{ h}^{-1}$ and 300°C . Reaction conditions: 0.1 g of catalyst (0.5 wt.\% of Pt), $P = 1 \text{ atm}$, molar ratio $\text{H}_2/\text{n-C}_{10} = 7$.

Table 3

Product distribution of *n*-decane hydroisomerization over different catalysts at 300 °C and WHSV = 6.6 h⁻¹.

Samples	Pt/SO.4Si	Pt/S-Merck	Pt/S-Mox	Pt/S-Mox300
Conversion ^a (%)	7.9	9.4	12.5	9.6
Mono-C ₁₀ (M)	5-MC ₉	0.5	0.7	0.6
	4-MC ₉	0.9	1.4	1.3
	2-MC ₉	2.4	3.0	2.5
	3-EC ₈	0.0	0.0	0.2
	3-MC ₉	2.0	2.7	2.4
	Total	5.8	7.5	7.0
Yield (%)	Di-C ₁₀ (B)	0.4	0.5	1.1
Cracking	C ₉	0.0	0.0	0.0
	C ₈	0.0	0.0	0.0
	C ₇	0.4	0.2	0.5
	C ₆	0.3	0.3	0.4
	C ₅	0.5	0.4	1.1
	C ₄	0.5	0.4	1.0
	C ₃ -C ₁	0.0	0.0	0.1
	Total	1.7	1.4	3.6
				1.8

^a Reaction conditions: 0.1 g of catalyst (0.5 wt.% of Pt), P = 1 atm, molar ratio H₂/n-C₁₀ = 7.

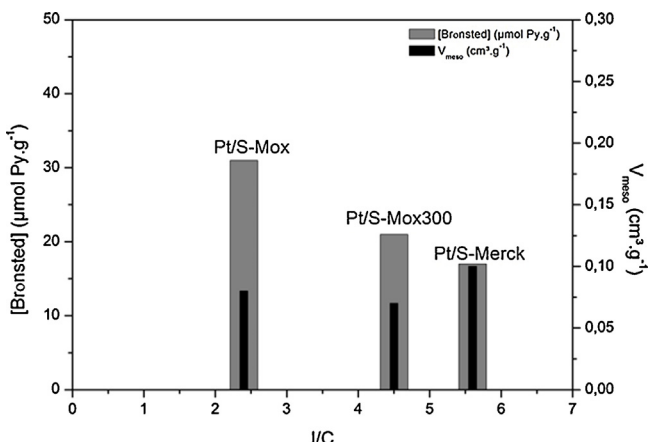


Fig. 8. Ratio of the sum of isomerization and cracking products (I/C) on Pt/SO.4Si, Pt/S-Mox, Pt/S-Mox300 and Pt/S-Merck samples at WHSV = 6.6 h⁻¹ and 300 °C of as a function of concentration of Brønsted acid sites and the mesopores volume, V_{meso} .

case of S-Merck sample. However the most relevant effect seems to be the acidity, which is related with the differences in the surface chemistry of the carbon templates, as discussed before. Indeed, the lower acidity presented Pt/S-Merck as a consequence of higher pH_{pzc} presented by Merck carbon (see Fig. 2) hinders the occurrence of a second isomerization step and the formation of cracking products.

These results clearly point out to the influence of the surface chemistry of the carbon matrix in the final acidity properties of the hierarchical SAPO-11 material and its consequences on the catalytic behavior.

4. Conclusions

The commercial Merck and oxidized (Mox and Mox300) carbon templates, added during the preparation of the gels, allowed to obtain hierarchical SAPO-11 materials with both micro and mesopores. The external surface area, A_{ext} , and mesopores volume, V_{meso} , increased for all samples when compared with the carbon-free SAPO-11. The subsequent SAPO-11 materials synthesized showed cavities, irregular in shape and size, formed during carbon combustion.

The oxidant acid and heat treatments induced an increase of oxygenate surface groups but showed not changes the external surface area and mesopore volume, when comparing with the samples synthesized with commercial Merck carbon. The results show that carbon oxidation treatments affect the matrix surface groups, resulting in the modification of the SAPO-11 gel chemistry. The addition of carbon matrix templates caused a decrease in the acidity for all samples, especially for the one synthesized with Merck carbon.

The *n*-decane hydroisomerization results show that the mesoporosity developed during the carbon templated synthesis was enough to improve the catalytic conversion of the hierarchical materials. The higher yields in the most valuable monobranched isomers, along with a reduction in cracking products was obtained for Pt/S-Merck due to a joint effect of mesoporosity increase and, most relevantly, a decreases on the acidity caused by the interaction with the surface chemical groups of the carbon matrix with higher pH_{pzc}.

In spite of solid templates have been reported in the literature as inert materials this preliminary study shows that the modification of the surface chemistry of the carbons seems to promote interactions with the synthesis gel, resulting in the production of SAPO-11 materials with different acid properties, with enhanced catalytic behavior.

A more detailed study, where several types of carbons with distinct surface chemistry properties were used as templates is in progress in order to deeply understand the interactions between the solid matrix and the gel synthesis, with direct influence on the final properties of the hierarchical materials.

Acknowledgments

The authors thank Portuguese FCT for financial support (SFRH/BD//73234/2010 and SFRH/BPD/91397/2012), Prof. Teresa Duarte for access to the XRD facility (CONC-REEQ/670/2001) and Prof. João Rocha for NMR experiments.

References

- [1] A. Corma, Chem. Rev. 97 (1997) 2373–2420.
- [2] M. Guisnet, F.R. Ribeiro, Les Zeolithes, Un nanomonde au Service de la catalyse, EDP Science, 2006.
- [3] S. Lopez-Orozco, A. Inayat, A. Schwab, T. Selvam, W. Schwieger, Adv. Mater. 23 (2011) 2602–2615.

- [4] R. Chal, C. Gérardin, M. Bulut, S. van Donk, *ChemCatChem.* 3 (2011) 67–81.
- [5] C.J.H. Jacobsen, C. Madsen, J. Houzvicka, I. Schmidt, A. Carlsson, *J. Am. Chem. Soc.* 122 (2000) 7116–7117.
- [6] B.M. Lok, C.A. Messina, R.L. Patton, R.T. Gajek, T.R. Cannan, E. Flanigen, 1984, US Patent 4 440 871.
- [7] T. Blasco, A. Chica, A. Corma, W. Murphy, J. Agundez Rodriguez, J. Perez Pariente, *J. Catal.* 242 (2006) 153–161.
- [8] J.A. Martens, P.A. Jacobs, J. Weitkamp, *Appl. Catal. B* 20 (1986) 239–281.
- [9] J.A. Martens, G. Vanbutsele, P.A. Jacobs, J. Denayer, R. Ocakoglu, G. Baron, J.A. Muñoz Arroyo, J. Thybaut, G.B. Marin, *Catal. Today* 65 (2001) 111–116.
- [10] C. Moreno-Castilla, F. Carrasco-Marín, F.J. Maldonado-Hódar, *Carbon* 36 (1998) 145–151.
- [11] A.F. Pérez-Cadenas, F.J. Maldonado-Hódar, C. Moreno-Castilla, *Carbon* 41 (2003) 473–478.
- [12] R. Bértolo, Â. Martins, J.M. Silva, F. Ribeiro, F.R. Ribeiro, A. Fernandes, *Micro-porous Mesoporous Mater.* 143 (2011) 284–290.
- [13] W. Lutz, R. Kurzhals, S. Sauerbeck, H. Toufar, J.C. Buhl, T. Gesing, W. Altenburg, C. Jäger, *Microporous Mesoporous Mater.* 132 (2010) 31–36.
- [14] M. Alfonzo, J. Goldwasser, C.M. López, F.J. Machado, M. Matjushin, B. Méndez, M.M. Ramírez de Agudelo, *J. Mol. Catal. A Chem.* 98 (1995) 35–48.
- [15] C.A. Emeis, *J. Catal.* 141 (1993) 347–354.
- [16] J. Perez-Ramirez, C.H. Christensen, K. Egeblad, J.C. Groen, *Chem. Soc. Rev.* 37 (2008) 2530–2542.
- [17] S. Zhang, S.-L. Chen, P. Dong, *Catal. Lett.* 136 (2010) 126–133.
- [18] S.J. Miller, *Microporous Mater.* 2 (1994) 439–449.
- [19] F. Marques Mota, C. Bouchy, E. Guillou, A. Fécaut, N. Bats, J.A. Martens, *J. Catal.* 301 (2013) 20–29.
- [20] H. Deldari, *Appl. Catal. A Gen.* 293 (2005) 1–10.
- [21] J. Hancsók, S. Kovács, G. Pölczmann, *Top. Catal.* 54 (2011) 1094–1101.